Interactions of DNR1 with the apoptotic machinery of *Drosophila melanogaster*

David A. Primrose, Sidharth Chaudhry, A. George D. Johnson, Adam Hrdlicka, Anja Schindler, Dave Tran and Edan Foley*

Department of Medical Microbiology and Immunology, University of Alberta, Edmonton AB, T6G 2S2, Canada

*Author for correspondence (e-mail: efoley@ualberta.ca)

Accepted 23 January 2007
Journal of Cell Science 120, 1189-1199 Published by The Company of Biologists 2007
doi:10.1242/jcs.03417

Summary

Caspases are crucial activators of apoptosis and NF-κB signaling in vertebrates and invertebrates. In *Drosophila*, the caspase-9 counterpart Dronc is essential for most apoptotic death, whereas the caspase-8 homolog Dredd activates NF-κB signaling in response to gram-negative bacterial infection. The mechanics of caspase regulation are conserved and include the activities of a family of inhibitor of apoptosis (IAP) proteins. The RING-domain-bearing protein Defense repressor 1 (Dnr1), blocks ectopic Dredd-mediated induction of an NF-κB reporter in the *Drosophila* S2 cell line. In this study, we present novel data indicating that Dnr1 impacts on Dronc-dependent regulation of the apoptotic program. We show that depletion of Dnr1 results in elevated Dronc protein levels, which translates to increased caspase activation and activity upon induction of apoptosis. Conversely, we demonstrate that overexpression of Dnr1 blocks apoptotic caspase activity and prevents induction of apoptosis in tissue culture assays. Furthermore, we show that Dnr1 overexpression significantly reduces Dronc protein levels and identify the domains of Dnr1 necessary for these effects. From these data, we propose that Dnr1 inhibits initiator caspases in S2 cells.

Supplementary material available online at
http://jcs.biologists.org/cgi/content/full/120/7/1189/DC1

Key words: Dnr1, Dronc, Apoptosis, Caspases, IAP

Introduction

All metazoans remove unwanted or potentially deleterious cells through a process known as apoptosis or programmed cell death (Horvitz, 1999; Jacobson et al., 1997). Apoptosis contributes to the definition of adult structures during development. In addition, apoptosis plays a crucial role in the long-term survival of metazoans by destroying pre-cancerous or virally infected cells as well as lymphocytes that produce auto-reactive antibodies (Baehrecke, 2002; Green and Evan, 2002; Opferman and Korsmeyer, 2003; Raff, 1992; Vaux and Flavell, 2000; Vaux and Korsmeyer, 1999). Furthermore, excess apoptosis has been linked to a number of debilitating conditions, such as neurodegenerative disorders (Thompson, 1995; Yuan and Yankner, 2000). Thus, there is a clear need to identify the regulatory mechanisms that govern execution of the apoptotic program.

Pioneering work in the model organism *C. elegans* (Yuan et al., 1993) revealed that apoptosis is mediated by the activity of a family of cysteinyl aspartate proteases (caspases). Subsequent work in other systems demonstrated that caspases are universal mediators of apoptosis. Caspases are zymogens characterized by N-terminal pro-domains, which are followed by large and small catalytic subunits (Shi, 2002). Typically, caspases are divided into two categories – initiator and effector caspases. Initiator caspases are distinguished by long N-terminal pro-domains, whereas effector caspases are characterized by short pro-domains. Pro-apoptotic signals typically trigger the assembly of macromolecular complexes containing initiator caspases. For example, cytotoxic stress in mammals induces release of mitochondrial cytochrome *c* into the cytoplasm, which complexes with the adaptor protein Apaf-1, and dATP and caspase-9 to form the apoptosome (Li et al., 1997; Rodriguez and Lazebnik, 1999; Saleh et al., 1999; Zou et al., 1999). The apoptosome initiates apoptosis through caspase-9-mediated cleavage of short inhibitory N-terminal pro-domains from effector caspases such as caspase-3. Effector caspases then undergo a defined series of structural rearrangements that include proteolytic cleavage between the large and small subunits and dimerization, resulting in their activation. Once active, effector caspases cleave a large number of cellular substrates, thereby ushering in the defining molecular and morphological features of apoptosis.

Work in model organisms has revealed that the molecular pathways governing caspase activation and activity are evolutionarily conserved. For example, developmental or stress-induced apoptosis in *Drosophila* triggers activation of Dronc (caspase-9 homolog), which interacts with Dark (*Drosophila* Apaf-1 homolog) and subsequently activates Drice (caspase-3 homolog) to trigger apoptotic death (Chew et al., 2004; Daish et al., 2004; Dorstyn et al., 1999; Fraser and Evan, 1997; Fraser et al., 1997; Kanuka et al., 1999; Kilpatrick et al., 2005; Muro et al., 2004; Quinn et al., 2000; Rodriguez et al., 1999; Xu et al., 2005; Zhou et al., 1999). Thus, genetically accessible organisms such as *Drosophila* have emerged as potent systems for deciphering apoptosis.

The inhibitor of apoptosis (IAP) protein family is an evolutionarily conserved family of caspase inhibitors that has been extensively characterized in *Drosophila*. IAPs were first identified in baculoviruses and have since been found in a range of multicellular organisms (Deveraux and Reed, 1999;

Hay, 2000; Vaux and Silke, 2005). All IAPs contain one or more baculovirus IAP repeat (BIR) motifs, although, not all BIR-containing proteins are caspase regulators. For example, IAP1 of *C. elegans* is dispensable for regulation of the apoptotic program, whereas it has established roles in cytokinesis (Fraser, 1999). In the case of caspase-inhibitory IAPs, BIR motifs are involved in IAP-caspase interactions, either directly or through coordination of adjacent residues (Shi, 2002). In addition to BIR motifs, caspase-inhibitory IAPs contain C-terminal RING domains. RING domains are E3 type ubiquitin ligases that target substrates for proteasomal degradation by polyubiquitylation. Whereas RING domains are found in a large number of proteins, the RING domains in IAPs are characterized by a distinct spacing of crucial cysteine residues, suggesting a functional specialization. Recently, the RING-domain-bearing CARP protein family has been identified as an inhibitor of human caspase-8 and caspase-10 (McDonald and El-Deiry, 2004). Whereas the RING domain of CARP proteins is highly similar to established caspase-inhibitory IAPs, CARPs lack a BIR motif, suggesting that RING domains alone are capable of inhibiting caspases.

Several IAPs are known to regulate their own stability through RING-domain-mediated auto-ubiquitination and are postulated to also target caspases for destruction by ubiquitylation (Vaux and Silke, 2005). One of the best characterized IAPs is *Drosophila* IAP1 (DIAP1). DIAP1 is an essential regulator of apoptosis and DIAP1 loss results in extensive apoptosis both in whole animals and tissue culture assays (Hay et al., 1995; Kaiser et al., 1998; Muro et al., 2002; Rodriguez et al., 2002; Wang et al., 1999). DIAP1 physically interacts with and ubiquitinates Dronc (Chai et al., 2003; Meier et al., 2000; Wilson et al., 2002). Mutations affecting the RING domain of DIAP1 are embryonic lethal, confirming that the RING domain is essential for DIAP1 in vivo function (Goyal et al., 2000; Lisi et al., 2000; Wang et al., 1999; Yoo et al., 2002). Pro-apoptotic molecules such as Grim, Reaper and Hid counter DIAP1 activity by disrupting DIAP1-Dronc interactions to liberate active Dronc and thereby induce cell death (Chai et al., 2003; Chen et al., 2004; Chen et al., 1996; Grether et al., 1995; Vucic et al., 1998; White et al., 1994; White et al., 1996; Zachariou et al., 2003).

In addition to the established roles of caspases in apoptosis recent studies have demonstrated additional functions for caspases in metazoans. For example, *Drosophila* caspases have non-apoptotic roles in spermatid differentiation (Arama et al., 2003; Huh et al., 2004). Additionally, the *Drosophila* caspase-8 homolog Dredd is essential for activation of the innate immune response to infection with gram-negative bacteria (Leulier et al., 2000; Stoven et al., 2000; Stoven et al., 2003). Infection-induced Dredd activation results in cleavage and concomitant activation of an NF-κB transcription factor family member Relish at a caspase consensus cleavage site. The role of caspase-8 in immune signaling appears conserved, because mammalian caspase-8 is required for lymphocyte activation in humans and mice (Chun et al., 2002; Salmena et al., 2003; Su et al., 2005).

Defense repressor 1 (Dnr1) was identified as an inhibitor of Dredd activity in the absence of a microbial insult in *Drosophila* S2 cells (Foley and O'Farrell, 2004). Dnr1 is 677 amino acids long, with an N-terminal FERM domain followed by a region rich in glutamine and serine residues, a central FERM_C motif and a C-terminal RING domain. Inactivation of Dnr1 in vitro resulted in ectopic production of a Relish-dependent reporter, which was suppressed by co-inactivation of either Dredd or Relish, suggesting that Dnr1 inhibits Dredd-mediated activation of Relish. Although it lacks a BIR motif, the C-terminal RING domain on Dnr1 has extensive similarity to the RING domains in other IAPs. Dnr1 is an unstable protein and this lack of stability requires an intact RING domain, indicating that, similar to other IAPs, Dnr1 regulates its own stability. Additionally, Dnr1 protein levels are affected by Dredd activity. Activation of Dredd results in transitory stabilization of Dnr1, whereas inactivation of Dredd, either by p35 overexpression, z-VAD-fmk incubation or RNA interference (RNAi) targeting Dredd diminishes Dnr1 levels. These data suggest the possibility of a feedback loop between Dnr1 and Dredd, where Dredd activation results in accumulation of its own inhibitor Dnr1, which then blocks Dredd activity after the passing of an infection.

In this study we explore the interaction of Dnr1 with the *Drosophila* apoptotic apparatus using in vitro assays, and present novel data suggesting an inhibitory effect of Dnr1 on Dronc. We show that depletion of Dnr1 from S2 cells results in an increase of Dronc protein levels and apoptosis-dependent caspase activation and activity. Additionally, we demonstrate that overexpression of Dnr1 in S2 cells depletes Dronc protein levels in a RING domain-dependent manner and blocks induction of apoptosis in vitro. From these data, we propose that Dnr1 inhibits the *Drosophila* initiator caspases Dredd and Dronc.

Results

Dronc and Drice are essential for induction of apoptosis in *Drosophila* S2 cells

To investigate potential roles for Dnr1 in apoptosis, we established a series of assays to monitor apoptotic progression in the *Drosophila* S2 cell line. The nucleic acid synthesis inhibitor actinomycin D is an established inducer of apoptosis, and incubation of S2 cells with actinomycin D for 6 hours results in extensive membrane blebbing – a morphological hallmark of apoptosis (Fig. 1B). Approximately 40% of S2 cells showed signs of membrane blebbing 6 hours after exposure to actinomycin D (Fig. 1C). We measured the caspase activity of lysates prepared from actinomycin-D-treated S2 cells towards a series of established caspase substrates. We detected robust cleavage of DEVD and YEVD peptide substrates and a weaker but reproducible cleavage of VEID, IETD and LEHD substrates (Fig. 1D).

To identify the caspases required for apoptotic DEVDase and YEVDase activity, we treated S2 cells with double-stranded RNAs (dsRNAs) targeting six individual *Drosophila* caspases (Dronc, Drice, Dredd, Dcp-1, Decay and Damm) and measured actinomycin-D-dependent caspase activity in the respective cultures. The dsRNAs were taken from a library of previously described dsRNAs (Foley and O'Farrell, 2004). We confirmed through western blot analysis for Dronc and Drice, and a functional assay for Dredd that the respective dsRNAs effectively decreased the levels of the targeted proteins (data not shown). We did not detect *damm* transcript in S2 cells by real-time PCR analysis, indicating that Damm is not expressed in S2 cells (data not shown). We also confirmed by real-time analysis that dsRNA targeting *decay* effectively decreased *decay*

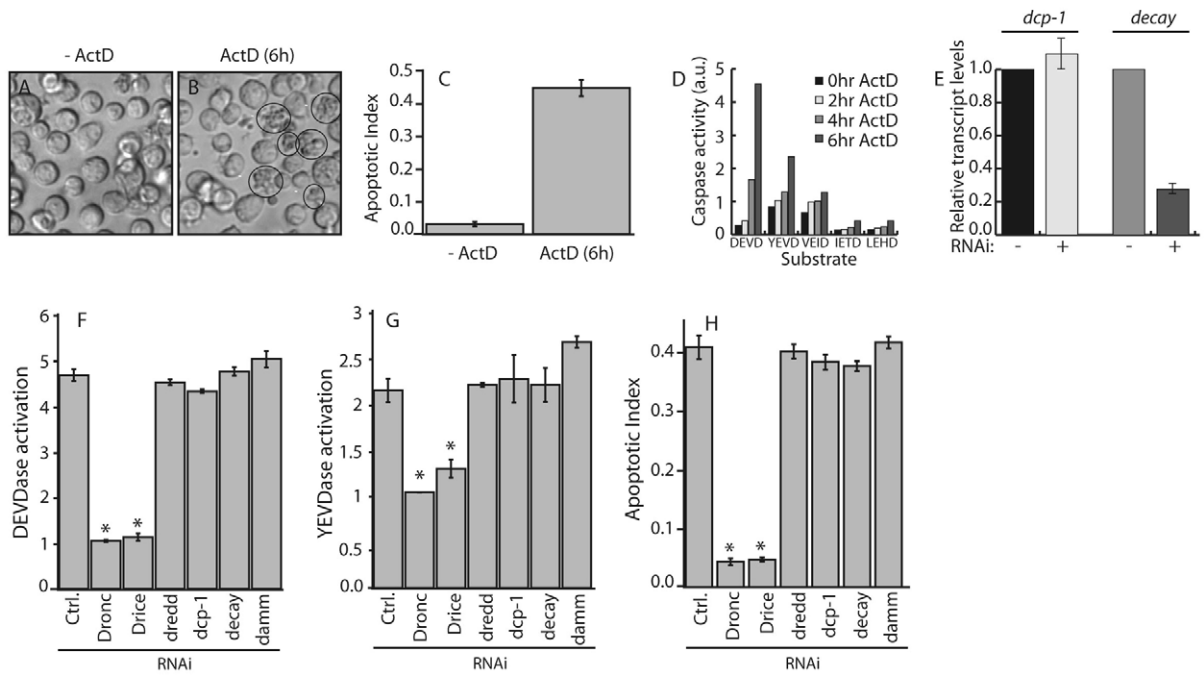

Fig. 1. Dronc and Drice are essential for apoptosis in S2 cells. (A,B) DIC images of control S2 cells (A) and S2 cells treated with actinomycin D for 6 hours (B). Apoptotic cells undergoing membrane blebbing, a characteristic of apoptosis, are circled in (B). (C) Quantification of the apoptotic index of control S2 cells (column 1) and S2 cells incubated with actinomycin D for 6 hours (column 2). Results are the mean of three independent experiments and error bars indicate standard errors. (D) Time course of caspase activity towards peptide substrates in lysates from S2 cells treated with actinomycin D, which induces a robust increase in DEVDase and YEVDase activity. (E) Real-time PCR quantification of *dcp-1* (columns 1 and 2) and *decay* (columns 3 and 4) transcript levels in control S2 cells (columns 1 and 3) compared with cells incubated for 72 hours with the respective dsRNA (columns 2 and 4). Dcp-1 dsRNA has no effect on *dcp-1* transcript levels whereas Decay dsRNA reduces *decay* transcript levels by 72%. Results are the mean of three independent measurements and error bars indicate standard errors. (F) DEVDase activity of lysates from actinomycin-D-treated (6 hours) control S2 cells and S2 cells incubated with dsRNA targeting the indicated caspases. DEVDase activity is expressed as a fold-change compared with lysates from the corresponding cell population not treated with actinomycin D. Results are the mean of three independent experiments and error bars indicate standard errors. **P*<0.01, values that differ significantly from untreated cells. (G) YEVDase activity of lysates from actinomycin-D-treated control S2 cells and S2 cells incubated with dsRNA targeting the indicated caspases. YEVDase activity is expressed as a fold-change compared with lysates from the corresponding cell population not treated with actinomycin D. **P*<0.01, values that differ significantly from untreated cells. Results are the mean of three independent experiments and error bars indicate standard errors. RNAi of Dronc or Drice significantly reduces DEVDase and YEVDase activity compared with control S2 cells. (H) Apoptotic indices of actinomycin-D-treated control S2 cells and S2 cells incubated with dsRNA targeting the indicated caspases. Dronc and Drice dsRNA block the onset of actinomycin-D-mediated apoptosis. Results are the mean of three independent experiments and error bars indicate standard errors. **P*<0.01, values that differ significantly from untreated cells.

transcript levels (Fig. 1E). Interestingly, Dcp-1 dsRNA had no measurable impact on the *dcp-1* transcript (Fig. 1E). Inspection of the dsRNA sequence revealed that the reported dsRNA fails to target *dcp-1*. Instead, the dsRNA targets a section of genomic DNA upstream of the *dcp-1* transcript. Thus, we conclude that our RNAi analysis effectively addresses involvements of Dronc, Drice, Decay and Dredd in apoptosis, whereas Damm is unlikely to contribute to apoptosis in S2 cells.

We observed a substantial drop in actinomycin-D-induced caspase activity after Dronc or Drice RNAi, whereas all other treatments failed to impact on DEVDase or YEVDase activity (Fig. 1F,G). In addition, dsRNA targeting Dronc or Drice prevented actinomycin-D-mediated apoptosis (Fig. 1H). Thus, we conclude that Dronc and Drice are essential for actinomycin-D-induced apoptosis in S2 cells, and that both caspases are the driving force behind apoptotic DEVDase and YEVDase activity. We note that our data are consistent with previous reports demonstrating a Dronc-Drice hierarchy in *Drosophila* apoptosis (for a review, see Hay and Guo, 2006).

Dnr1 regulates Dronc protein levels

Entry into apoptosis is characterized by Drice-dependent cleavage of Dronc at residue D135, yielding the apoptotic Pr2 isoform of Dronc, which lacks the pro-domain. Auto-processing of Dronc at residue E352 generates the large (L) and small (S) catalytic subunits (Fig. 2B) (Muro et al., 2004). To measure the consequence of Dnr1 loss on apoptotic progression in S2 cells, we treated S2 cells with dsRNA targeting Dnr1 and induced apoptosis three days later with actinomycin D. We confirmed by real-time PCR analysis that Dnr1 dsRNA significantly decreased *dnr1* transcript levels within 72 hours (Fig. 2A). We then measured full-length Dronc, Pr2 and large-Dronc protein levels in lysates prepared from control S2 cells (Fig. 2B lanes 2-5) or Dnr1 dsRNA-treated S2 cells (Fig. 2B lanes 7-10) at various times after exposure to actinomycin D. We reproducibly detected a significantly higher level of full-length Dronc in S2 cells treated with Dnr1 dsRNA than in control S2 cells prior to addition of actinomycin D (Fig. 2B). On average, there was

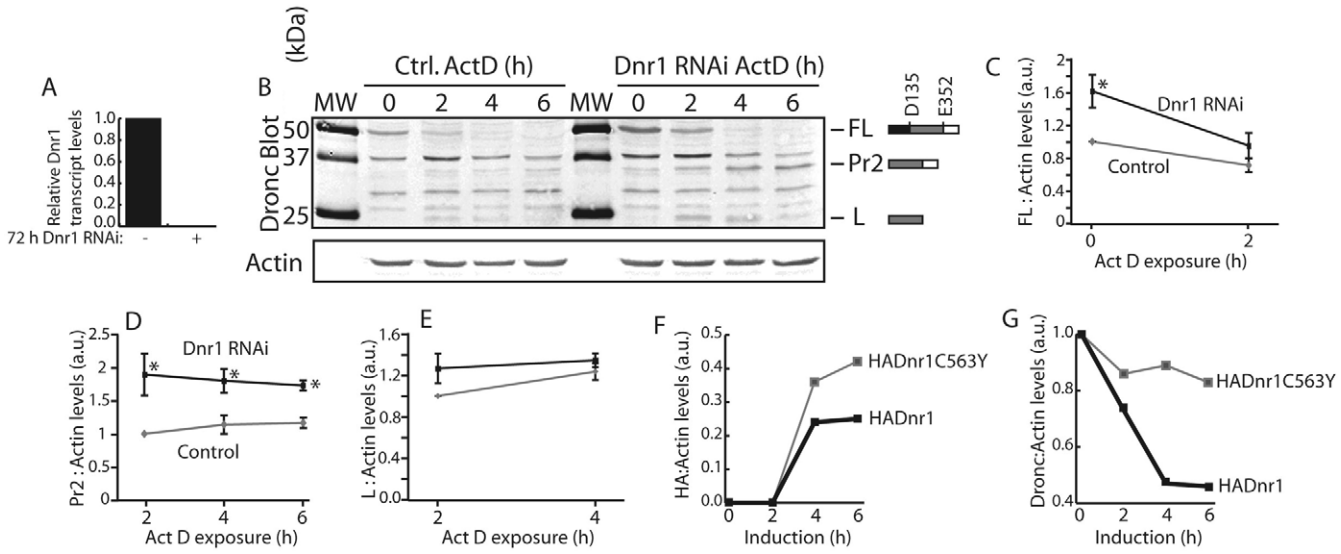

Fig. 2. Dnr1 affects Dronc protein levels. (A) Real-time PCR measurement of *dnr1* transcript levels in control S2 cells (column 1) and S2 cells incubated with Dnr1 dsRNA for 72 hours (column 2). *dnr1* transcript levels were normalized to actin transcript levels in both samples. Dnr1 dsRNA decreases *dnr1* transcript levels by greater than 95% within three days. (B) Western blot analysis of Dronc protein in lysates from control S2 cells (lanes 2-5) and S2 cells incubated with Dnr1 dsRNA (lanes 7-10). The cells were treated with actinomycin D and lysates harvested at the indicated periods. Molecular mass markers are shown in lanes 1 and 6, actin levels are shown as loading controls (lower panel) and the full-length (FL), Pr2 and L Dronc isoforms are indicated. (C-E) Quantification of the (C) full-length (FL), (D) Pr2 and (E) large (L) forms of Dronc in control S2 cells or S2 cells treated with Dnr1 dsRNA. Dronc protein levels are normalized relative to actin protein levels. The Dronc:actin levels in control S2 cells at 0 hours actinomycin D treatment were assigned a value of 1 in (C) and the remaining Dronc:actin values are reported relative to this value. We detected a significant increase in full-length Dronc protein levels in S2 cells incubated with Dnr1 dsRNA compared with control cells in the absence of induction. Results are the mean of three independent experiments and error bars indicate standard errors. **P*<0.03, values that differ significantly from untreated cells. We also detected elevated levels of the Pr2 and large isoforms of Dronc in cells treated with Dnr1 dsRNA (D and E, respectively). Results are the mean of three independent experiments and error bars indicate standard errors. **P*<0.01, values that differ significantly from untreated cells. (F) Time course of induction of HADnr1 or HADnr1C563Y. HADnr1 and HADnr1C563Y levels are normalized to actin levels. (G) Levels of full-lenght Dronc at various times after induction of HADnr1 or HADnr1C563Y. Full-lenght Dronc levels are normalized to actin levels in both samples.

approximately 60% more full-length Dronc protein in S2 cells treated with Dnr1 dsRNA than in control S2 cells prior to addition of actinomycin D (Fig. 2C).

As anticipated, we observed a disappearance of full-length Dronc upon induction of apoptosis and appearance of the Pr2 and large isoforms (Fig. 2B). Interestingly, we observed significantly elevated levels of the Pr2 isoform of Dronc in S2 cells treated with Dnr1 dsRNA compared with control S2 cells (Fig. 2B,D). We also detected a mild increase in the levels of the large catalytic subunit of Dronc in apoptotic S2 cells pre-treated with Dnr1 dsRNA compared with control apoptotic S2 cells (Fig. 2E). Thus, we conclude that loss of Dnr1 results in elevated Dronc protein levels in S2 cells. As Dnr1 depletion results in elevated Dronc protein levels, we asked whether overexpression of Dnr1 decreases Dronc levels. To this end, we transfected S2 cells with expression plasmids that allow copper-inducible expression of N-terminally HA-tagged Dnr1 (HADnr1) or an HADnr1 variant where the RING domain has been inactivated by site-directed mutagenesis of a crucial cysteine residue (HADnr1C563Y). We detected approximately two-fold higher levels of HADnr1C563Y than HADnr1 6 hours after induction, consistent with a role for the RING domain in Dnr1 destruction (Fig. 2F). Interestingly, overexpression of HADnr1C563Y had little impact on Dronc protein levels, whereas overexpression of HADnr1 decreased Dronc protein levels by approximately 50% within 6 hours (Fig. 2G). In summary, loss of Dnr1 results in accumulation of Dronc protein, whereas overexpression of Dnr1 decreases Dronc protein levels. Combined, these data indicate a role for Dnr1 in regulating Dronc protein levels in S2 cells.

Depletion of Dnr1 sensitizes cells to induction of caspase activity

As Dnr1 depletion results in accumulation of Dronc protein, we tested whether Dnr1 depletion also results in elevation of Dronc-mediated apoptosis. A commercial antibody raised against the active form of caspase-3 detects Drice activation during apoptosis (Fig. 3A) (Yu et al., 2002). Actinomycin D treatment failed to result in the appearance of an active caspase-3 signal in S2 cells where Dronc or Drice were depleted by RNAi (Fig. 3B, lanes 7-10). By contrast, Dredd and Decay depletion failed to prevent appearance of the active caspase-3 signal (Fig. 3B, lanes 3-6). We believe that the signal does not correspond to Dronc because the signal requires Drice activity (an event that lies downstream of Dronc activiation). Thus, we propose that the active caspase-3 signal most probably corresponds to an active variant of Drice or Dcp-1. We monitored caspase-3 activation in actinomycin-D-treated control S2 cells and S2 cells treated with Dnr1 dsRNA. We detected an earlier and more intense

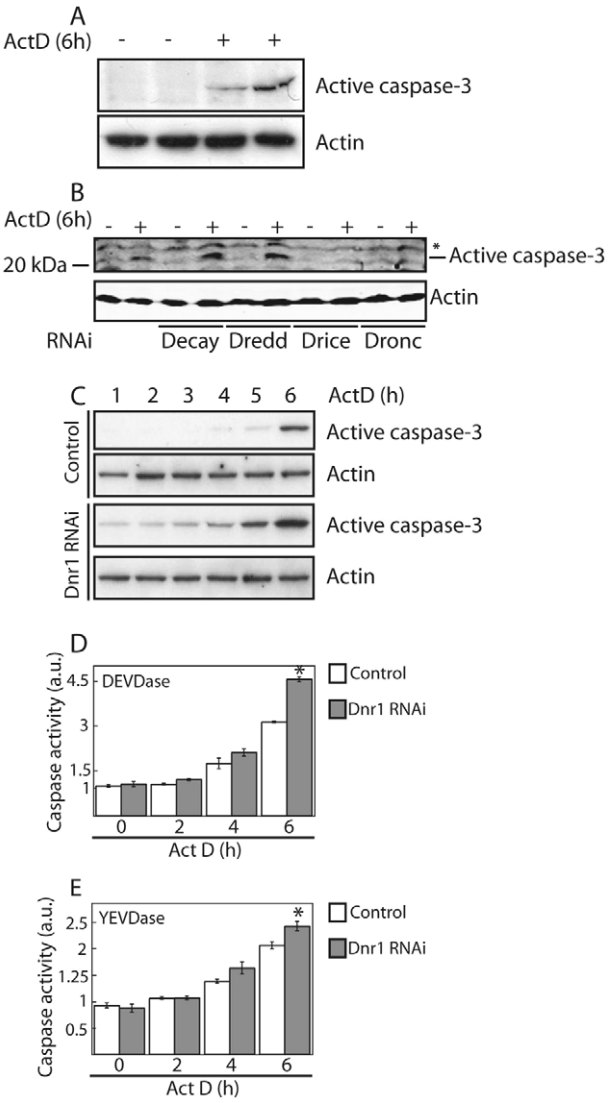

Fig. 3. Dnr1 RNAi enhances caspase activation and activity by actinomycin D in S2 cells. (A) Western blot analysis of lysates from control S2 cells and S2 cells incubated with actinomycin D using an antibody that detects active caspase-3 (upper panel). Both treatments were performed in duplicate. Actin levels are shown as a loading control (lower panel). Actinomycin D treatment results in the appearance of an active caspase-3 signal by 6 hours. (B) Western blot analysis of lysates from control S2 cells (lanes 1-2) decay dsRNA-treated cells (lanes 3-4), Dredd dsRNA-treated cells (lanes 5-6), Drice dsRNA-treated cells (lanes 7-8) and Dronc dsRNA-treated cells (lanes 9-10). Where indicated, cells had been incubated with actinomycin D for 6 hours. Lysates were probed with an active-caspase 3 antibody. An active caspase-3 signal is detected in S2 cells, as well as Dredd and Decay dsRNA-treated cells, whereas depletion of Drice or Dronc abrogates the signal. A crossreacting band is indicated by an asterisk. (C) Time course of caspase activation by actinomycin D in lysates from S2 cells (first panel) and lysates from S2 cells treated with Dnr1 dsRNA (third panel). Actin levels are shown as a loading control for both samples (second and fourth panel, respectively). Dnr1 RNAi results in an earlier and stronger appearance of the active caspase isoform at all times measured. (D,E) Time courses of DEVDase (D) and YEVDase (E) activity from actinomycin-D-treated lysates from control S2 cells and Dnr1 RNAi treated S2 cells. Results are the mean of three independent experiments and error bars indicate standard errors. *P<0.01, values that differ significantly from untreated cells. Dnr1 depletion results in a significant increase of caspase activity in response to actinomycin D.

accumulation of the active caspase-3 isoform at all time points investigated in Dnr1 dsRNA-treated cells compared with the control cells (Fig. 3C).

To confirm that RNAi of Dnr1 enhanced actinomycin-D-induced caspase activity we compared the DEVDase and YEVDase activity profiles of actinomycin-D-treated control S2 cells with actinomycin-D-treated S2 cells where Dnr1 had been depleted through RNAi. Whereas the basal DEVDase-YEVDase level was similar in both cells types, exposure to actinomycin D significantly elevated the DEVDase and YEVDase activity of S2 cells treated with Dnr1 dsRNA compared with control S2 cells (Fig. 3D,E). We note that in our assays we detect caspase-3 activation in Dnr1 dsRNA-treated cells prior to an accumulation of DEVDase or YEVDase activity and suspect that this reflects differences in the sensitivities of the two assays.

Depletion of Dnr1 sensitizes cells to induction of apoptosis

To determine the consequences of Dnr1 depletion for onset of apoptosis, we monitored the apoptotic index of control S2 cells, GFP dsRNA-treated and Dnr1 dsRNA-treated S2 cells after treatment with actinomycin D. We noticed a significant elevation of the apoptotic index of Dnr1 dsRNA-treated cells compared with control S2 cells or GFP dsRNA-treated S2 cells at high concentrations of actinomycin D (0.1 and 1 μM, Fig. 4B,C). In addition, we noticed a much greater induction of apoptosis in Dnr1 dsRNA-treated cells at concentrations of actinomycin D that barely induced apoptosis in control S2 cells or GFP dsRNA-treated S2 cells (Fig. 4A). The apoptotic index of Dnr1 dsRNA-treated S2 cells was more than double that of control S2 cells 6 hours after exposure to 0.01 μM actinomycin D. In summary, depletion of Dnr1 results in elevated caspase activation and activity, which corresponds to an elevation in apoptotic induction.

Dnr1 overexpression in S2 cells prevents induction of apoptosis

To further probe the effects of Dnr1 on apoptosis we established a series of S2 cell lines that constitutively express HADnr1 or HADnr1C563Y. Levels of HA-Dnr1C563Y were considerably higher than the levels of HADnr1 in all cell lines tested (Fig. 5A, and data not shown), consistent with a role for the RING domain in downregulating Dnr1 protein levels. We measured the DEVDase, YEVDase, VEIDase, IETDase and LEHDase activity from actinomycin-D-treated S2 cells, and S2 cells that stably express HADnr1 or HADnr1C563Y (Fig. 5B). Although we detected a robust increase in the caspase activity of S2 cells or the HADnr1C563Y-expressing line upon actinomycin D treatment, caspase activity was essentially at background levels in HADnr1-expressing cells for all substrates tested. The failure of HADnr1C563Y-expressing cells to block caspase activity compared with HADnr1-expressing cells is not a consequence of lower levels of the C563Y mutant form, because inactivation

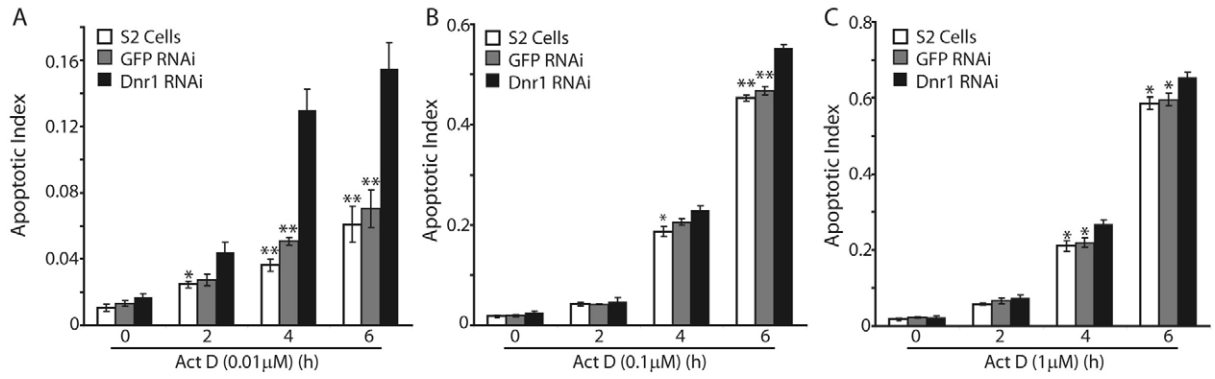

Fig. 4. Dnr1 depletion sensitizes cells to induction of apoptosis. Control S2 cells, GFP dsRNA-treated S2 cells or Dnr1 dsRNA-treated S2 cells were incubated with 0.01, 0.1 or 1 μM actinomycin D (A-C, respectively) and the apoptotic index of the different cell populations were determined as indicated. Results are the mean of three independent experiments and error bars indicate standard errors. ***P*<0.01, values that differ significantly from Dnr1 dsRNA-treated cells; **P*<0.05, values that differ significantly from Dnr1 dsRNA-treated cells. Dnr1 RNAi results in an elevated apoptotic index of actinomycin-D-treated S2 cells compared with control S2 cells or GFP dsRNA-treated S2 cells.

of the RING domain dramatically increases the levels of HADnr1C563Y (Fig. 5A). We also found that overexpression of Dnr1 essentially blocked actinomycin-D-induced apoptosis, whereas the level of apoptosis in HADnr1C563Y cells was identical to control S2 cells (Fig. 5C). We then expanded our studies to include other inducers of apoptosis and observed that overexpression of HADnr1 efficiently blocked induction of apoptosis by ultra-violet irradiation or cycloheximide treatment, whereas overexpression of HADnr1C563Y had no impact on apoptotic induction by either treatment (Fig. 5D). From these data, we conclude that Dnr1 overexpression blocks apoptotic induction by cytotoxic agents and this activity requires an intact RING domain on Dnr1.

Dnr1 rescues DIAP1 ablation-mediated apoptosis in a RING domain-independent manner

We expanded our studies further to include genetic inducers of apoptosis. DIAP1 is an essential inhibitor of apoptosis in *Drosophila* and loss of DIAP1 results in widespread apoptosis. As Dnr1 blocks induction of apoptosis by cytotoxic agents in S2 cells we investigated whether Dnr1 overexpression compensates for loss of DIAP1 in S2 cells. Consistent with previous reports, RNAi of DIAP1 induced widespread apoptosis in S2 cells within a day of addition of the dsRNA to the cell culture medium (Fig. 6A-C and supplementary material Movie 1). By contrast, the bulk of cells overexpressing HADnr1 failed to undergo apoptosis upon depletion of DIAP1 (Fig. 6D-F and supplementary material Movie 2), indicating that Dnr1 overexpression inhibits apoptosis in a DIAP1-independent manner. Surprisingly, we also noticed that overexpression of Dnr1C563Y blocked induction of apoptosis by RNAi of DIAP1 (Fig. 6G-I and supplementary material Movie 3). These data differ from our observation that the RING domain is essential for Dnr1-mediated inhibition of the induction of apoptosis by cytotoxic agents and suggest that mechanistic differences exist between apoptosis when induced by cytotoxic agents or DIAP1 dsRNA (see Discussion).

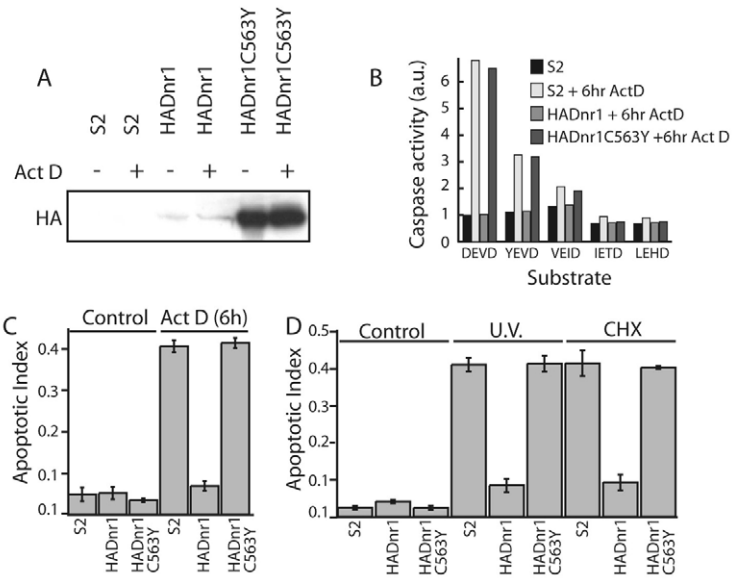

Fig. 5. Overexpression of Dnr1 blocks caspase activity and apoptosis in S2 cells. (A) Anti-HA western blot analysis of lysates from control S2 cells, S2 cells expressing HADnr1 and S2 cells expressing HADnr1C563Y treated with actinomycin D as indicated. Equal amount of lysate was loaded in each lane. The levels of HADnr1C563Y are considerably higher than HADnr1, consistent with a role for the RING domain in regulating Dnr1 stability. (B) Caspase activity assays in lysates from S2 cell, S2 cells treated with actinomycin D, HADnr1-expressing cells treated with actinomycin D and HADnr1C563Y-expressing cells treated with actinomycin D. HADnr1 expression blocks actinomycin-D-induced caspase activity, whereas the RING-domain-inactive version fails to impact on caspase activity. (C) Quantification of the apoptotic index of S2 cells, HADnr1-expressing S2 cells and HADnr1C563Y expressing S2 cells before (columns 1-3) or after exposure to actinomycin D (columns 4-6). Results are the mean of three independent experiments and error bars indicate standard errors. (D) Quantification of the apoptotic index of S2 cells, HADnr1-expressing S2 cells and HADnr1C563Y-expressing S2 cells before (columns 1-3) or after exposure to ultra-violet irradiation (columns 4-6) or cycloheximide (columns 7-9). Results are the mean of three independent experiments and error bars indicate standard errors.

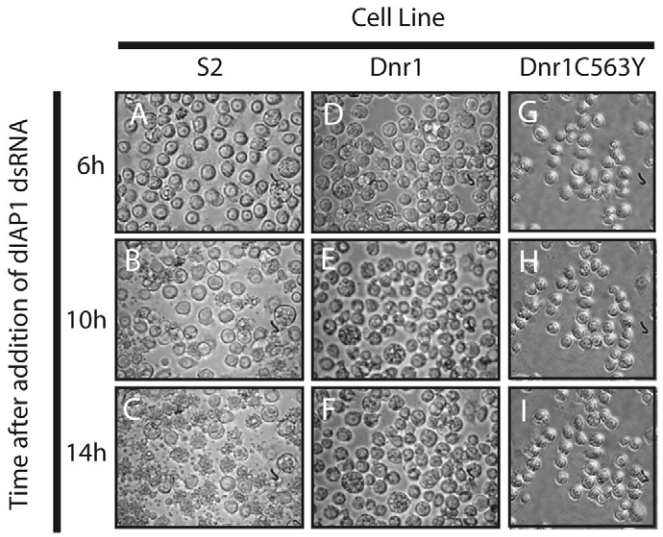

Fig. 6. (A-I) Time-lapse imaging of apoptotic progression in control S2 cells (A-C), HADnr1-expressing S2 cells (D-F) and HADnr1C563Y-expressing S2 cells (G-I). All cell lines were treated with dIAP1 dsRNA and imaged at the indicated time. Whereas DIAP1 depletion induces rapid apoptosis in control S2 cells, overexpression of Dnr1 or Dnr1C563Y suppresses the loss of DIAP1 phenotype.

Dnr1-mediated depletion of Dronc is pro-domain-independent

As Dnr1 appears to inhibit the initiator caspases Dredd and Dronc, we hypothesized that Dnr1 recognizes a structural feature of the larger pro-domain of initiator caspases. To test this we established an assay to quantify the ability of HADnr1-expressing cells to decrease Dronc protein levels. To this end, we transfected equal amounts of a plasmid that drives constitutive expression of N-terminally, 6×myc-tagged Dronc (6×mycDronc) into S2 cells, HADnr1-expressing S2 cells and HADnr1C563Y-expressing S2 cells and quantified levels of myc-tagged Dronc in the respective lines by western blot analysis. We detected three specific myc signals in all lines. One signal corresponds to full-length 6×mycDronc and two additional signals, at 32 kDa and 30 kDa, correspond to previously described isoforms of Dronc cleaved at aspartate 135 and 113, respectively (Muro et al., 2004). The levels of all three Dronc isoforms appeared lower in HADnr1-expressing S2 cells compared to control S2 cells or HADnr1C563Y-expressing S2 cells (Fig. 7A). To confirm this, we quantified the levels of the individual 6×mycDronc isoforms relative to a control protein (actin) in the individual cell lines. The levels of all three 6×mycDronc isoforms were significantly reduced in HADnr1-expressing cells compared with S2 cells, whereas HADnr1C563Y expression appeared to have no effect on any of the isoforms (Fig. 7B). These data are consistent with our above described observations that Dnr1 decreases Dronc protein levels in a RING-domain-dependent manner. We then transfected equal amounts of a plasmid that drives constitutive expression of an N-terminally, 6×myc-tagged Dronc isoform lacking the pro-domain (6×mycDroncΔPro) into S2, HADnr1 and HADnr1C563Y-expressing cells. Interestingly, we noticed a decrease in the levels of 6×mycDroncΔPro in HADnr1-expressing cells compared with both S2 control and HADnr1C563Y-expressing cells (Fig. 7C). Thus, we conclude that the pro-domain of Dronc is not essential for Dnr1-dependent depletion of Dronc protein levels.

Identification of domains within Dnr1 required for Dronc depletion

The primary sequence of Dnr1 contains an N-terminal FERM domain, a central glutamine/serine-rich region, a FERM_C

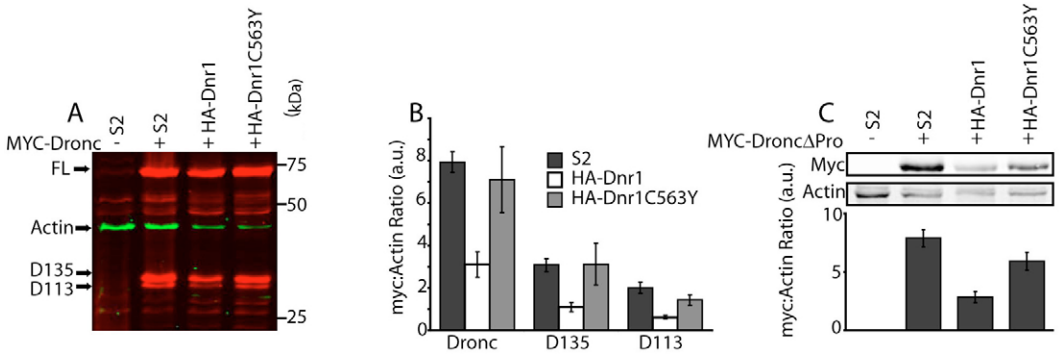

Fig. 7. Dnr1-dependent destruction of Dronc is pro-domain independent. (A) Western blot analysis of lysates from control S2 cells (lanes 1 and 2), and S2 cells constitutively expressing HADnr1 or HADnr1C563Y (lanes 3 or 4, respectively). The individual lines were transfected with a plasmid that drives expression of 6×mycDronc where indicated. Lysates were probed with anti-myc (red) and anti-actin antibodies (green). Three distinct Dronc isoforms were detected corresponding to the full-length (FL), D135 and D113 isoforms. Each isoform is indicated by an arrow. (B) Serial dilutions of lysates from S2 cells, HADnr1-expressing cells and HADnr1C563Y-expressing cells transfected with a 6×mycDronc expressing plasmid were analyzed by western blot analysis. The levels of the individual Dronc isoforms were quantified and normalized to the level of a control protein (actin). Results are the mean of three independent experiments and error bars indicate standard errors. The level of each Dronc isoform is significantly reduced in HADnr1-expressing cells compared with S2 cells, whereas HADnr1C563Y expression fails to impact on Dronc protein levels. (C) Equal amounts of a plasmid that drives expression of 6×mycDroncΔPro was transfected into S2 cells, HADnr1-expressing cells and HADnr1C563Y-expressing cells as indicated. The myc tag was visualized by western blot analysis (upper panel) and quantified (lower panel) relative to the levels of a control protein (actin, middle panel). Overexpression of Dnr1 decreases the levels of DroncΔPro, whereas the C563Y variant of Dnr1 has no significant impact on DroncΔPro levels. Results are the mean of three independent experiments and error bars indicate standard errors.

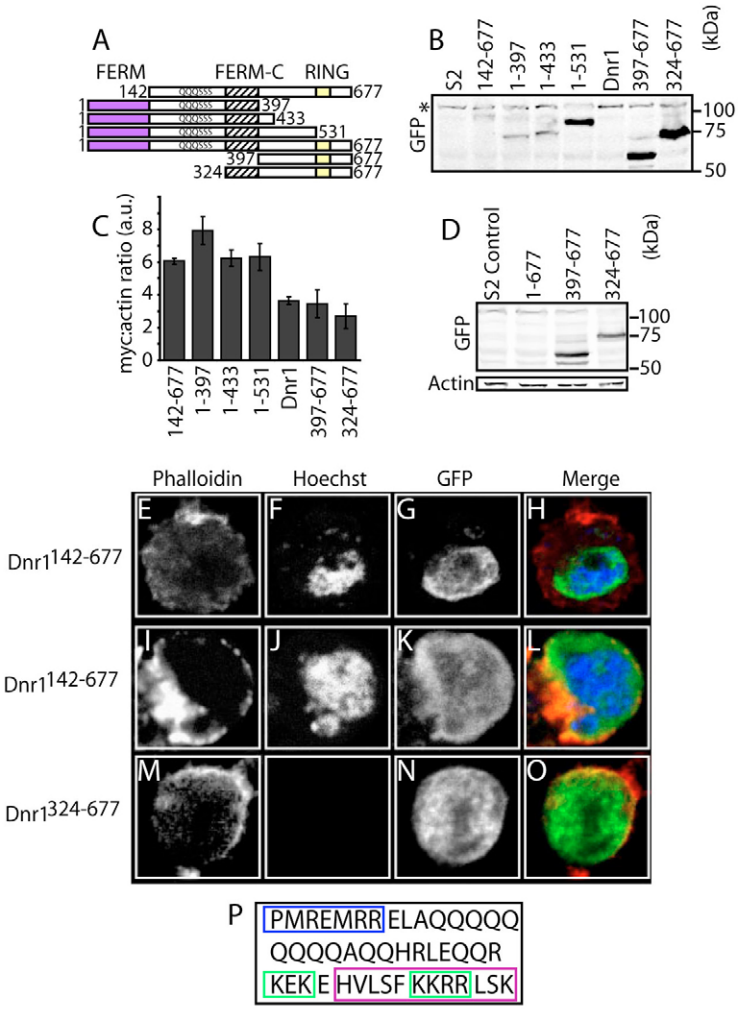

Fig. 8. Identifying functional domains within Dnr1. (A) Schematic representation of Dnr1, showing the FERM domain (purple), FERM_C motif (hatched) and RING domain (yellow). The indicated series of GFP-tagged expression constructs were prepared. (B) Anti-GFP western blot analysis of lysates from control S2 cells and a series of stable S2 cell lines expressing GFP-tagged versions of the indicated Dnr1 expression constructs. Molecular mass markers are indicated. A cross-reacting signal is indicated with an asterisk. (C) The individual stable lines were transfected with equal amounts of a plasmid that drives constitutive expression of 6×mycDronc and the ratio of full-length Dronc (C) to actin were quantified for the respective lines. Dnr1$^{324\text{-}677}$ and Dnr1$^{397\text{-}677}$-expressing cells diminished Dronc levels to a similar extent as wild-type Dnr1. Results are the mean of three independent measurements and error bars indicate standard errors. (D) Anti-GFP western blot of lysates from control S2 cells and S2 cells transfected with equal amounts of plasmids that drive expression of GFP-tagged versions of Dnr1, Dnr1$^{324\text{-}677}$ and Dnr1$^{397\text{-}677}$ as indicated. Molecular mass markers are indicated and actin levels are shown as loading controls. (E-O) Confocal images of S2 cells transfected with GFPDnr1$^{142\text{-}677}$ (E-L) and GFPDnr1$^{324\text{-}677}$ (M-O). In the merged images of panels H and O GFP is shown in green, DNA is visualized in blue and filamentous actin is labeled in red. In the merged image of panel L, GFP is shown in green, DNA is visualized in blue and the nuclear envelope is visualized in red with Alexa Fluor-568-labeled wheat germ agglutinin. Whereas GFPDnr1$^{324\text{-}677}$ is cytoplasmic GFPDnr1$^{142\text{-}677}$ is a nuclear protein, indicating the existence of an NLS between residues 142 and 324. Panels E-H and M-O are shown at 100× magnification and panels I-L are shown at 200× magnification. (P) Primary sequence of residues 150-193 in Dnr1. Three potential NLS are indicated, two are boxed blue or red boxes, a putative bipartite NLS is boxed green.

motif and a C-terminal RING domain (Fig. 8A). To identify the regions of Dnr1 required for Dronc depletion we generated a series of deletion constructs that sequentially remove each domain (Fig. 8A) and established a series of S2 cell lines that constitutively express N-terminally GFP-tagged versions of each construct. Western blot analysis confirmed that each line expressed the respective construct (Fig. 8B).

Consistent with a previous report, the full-length form of Dnr1 was barely detectable in whole-cell lysates (Fig. 8B, lane 6) and this is probably a reflection of RING-domain-dependent auto-ubiquitylation. We consistently noticed higher levels of Dnr1$^{324\text{-}677}$ and Dnr1$^{397\text{-}677}$ (mutant proteins lacking the N-terminal 324 and 397 residues, respectively) in our stable lines compared with full-length Dnr1 (Fig. 8B). From these data, we reasoned that N-terminal deletions stabilize Dnr1. To test this, we transfected equal amounts of plasmids that drive constitutive expression of GFP-tagged Dnr1, Dnr1$^{324\text{-}677}$ and Dnr1$^{397\text{-}677}$ into S2 cells (Fig. 8D). Western blot analysis confirmed that the N-terminal truncations were more stable than the full-length form, indicating that both the RING domain and N-terminal motifs are necessary for Dnr1-mediated auto-destruction.

We then transfected equal amounts of a 6×mycDronc-expressing plasmid into each of the cell lines and measured 6×mycDronc protein levels in lysates from the respective lines. As expected, Dronc protein levels were decreased in cells stably expressing full-length Dnr1 (Fig. 8C). Likewise, and in contrast to our observations with Dnr1, Dronc levels were decreased in cells expressing Dnr1$^{324\text{-}677}$ and Dnr1$^{397\text{-}677}$ constructs (Fig. 8C). All lines stably expressing Dnr1 C-terminal deletions that lack the RING domain failed to impact on Dronc protein levels (Fig. 8C). Surprisingly, we observed normal levels of Dronc in S2 cells stably expressing a Dnr1 construct that contained an intact RING domain but lacked the N-terminal FERM domain (Dnr1$^{142\text{-}677}$, Fig. 8C). As this construct has an intact RING domain, we reasoned that a FERM domain is also required for Dnr1-mediated destruction of Dronc. The FERM domain is a plasma-membrane-binding domain, thought to play structural and regulatory roles in the assembly and stabilization of specialized plasma membrane domains. We reasoned that the inability of Dnr1$^{142\text{-}677}$ to deplete Dronc probably reflected an alteration in the subcellular localization of Dnr1. To test this we compared the subcellular localization of Dnr1$^{142\text{-}677}$ with Dnr1$^{324\text{-}677}$, an N-terminal deletion construct that retains the ability to decrease Dronc protein levels. Confocal microscopy analysis revealed that Dnr1$^{142\text{-}677}$ is a nuclear protein, whereas Dnr1$^{324\text{-}677}$ displays a broad cytoplasmic localization (Fig. 8E-G). Examination of the primary sequence of Dnr1 identified several candidate nuclear localization sequences between

Table 1. Forward and reverse primer sequences used to generate pENTR/TOPO-D constructs for this study

Construct	Forward primer	Reverse primer
Dronc	CACCATGCAGCCGCCGGAGCT	TTCGTTGAAAAACCCGGG
DroncΔPro	CACCGTTCTATTGGAATCCGTCG	TTCGTTGAAAAACCCGGG
Dnr1	CACCATGTGGTGCATTGTCAACCTGCC	CTAGGCGGCCGTCGTAACCTTCG
$Dnr1^{142-677}$	CACCGAGTCGTCGCTGAAGGCCGACTGC	CTAGGCGGCCGTCGTAACCTTCG
$Dnr1^{1-531}$	CACCATGTGGTGCATTGTCAACCTGCC	CTACTCACGCGCCTCCTTCTCGC
$Dnr1^{1-433}$	CACCATGTGGTGCATTGTCAACCTGCC	CTACTTGAGATCCCGGGTAAACTG
$Dnr1^{1-397}$	CACCATGTGGTGCATTGTCAACCTGCC	CTACTTGGGCAGCTTGATCTCCAGC
$Dnr1^{324-677}$	CACCTACGGCGAGGAGCTCTTTAGC	CTAGGCGGCCGTCGTAACCTTCG
$Dnr1^{397-677}$	CACCCAGCCGATCGCCGCGGGCC	CTAGGCGGCCGTCGTAACCTTCG

N-terminally 6Xmyc-tagged Dronc and DroncΔPro were generated by recombining the respective TOPO constructs with pAMW (DGRC). N-terminally GFP-tagged Dnr1 and Dredd constructs were generated by left-right recombination of the respective TOPO constructs with pAGW (DGRC).

amino acids 150 and 194 (Fig. 8H). Thus, we conclude that Dnr1 requires both a cytoplasmic localization and an intact RING domain to deplete Dronc from S2 cells. Combined, these data identify key sequence motifs within Dnr1 required for auto-destruction and the regulation of Dronc protein levels.

Discussion

Caspases are essential mediators of life or death decisions in eukaryotes. In higher eukaryotes, initiator caspases, such as caspase-8 and 9, respond to extrinsic or intrinsic signals to induce apoptosis. Mammalian apoptosis is characterized by the integration of initiator caspases into macromolecular complexes, such as the apoptosome and the auto-proteolytic removal of long inhibitory pro-domains from the initiator caspases (Shi, 2002). Whereas Dronc requires Dark for activity (Kanuka et al., 1999; Kiessling and Green, 2006; Leulier et al., 2006; Mills et al., 2006; Rodriguez et al., 1999; Zhou et al., 1999; Zimmermann et al., 2002), it is not clear whether pro-apoptotic signals trigger apoptosome assembly and auto-proteolytic activation of Dronc. Instead, it appears that Dronc is retained in an inactive configuration by DIAP1 and that expression of the DIAP1 antagonists Reaper, Grim or Hid relieve DIAP1-mediated inhibition of Dronc. Inactivation of DIAP1 is sufficient to induce widespread apoptosis in whole animal and tissue culture models. Once active, mammalian and *Drosophila* initiator caspases cleave the short pro-domains from effector caspases and concomitantly activate effector caspases, such as Drice, in *Drosophila* or caspase-3, caspase-6 and caspase-7 in mammals. Active effector caspases cleave several hundred cellular substrates and ultimately usher cell death.

In this study, we focused on interactions between Dronc and the putative caspase inhibitor Dnr1. Our data confirm several previous reports that Dronc and Drice are essential for caspase activity and subsequent apoptosis in actinomycin-D-treated S2 cells, whereas other caspases (Dredd and Decay) appear dispensable. As a caveat, we point out that our assays failed to determine the extent to which Dcp-1 is involved in apoptosis, although recent reports suggest that Dcp-1 contributes together with Drice to execution of the apoptotic program (Muro et al., 2006; Xu et al., 2006). While we failed to detect a physical interaction between Dnr1 and Dronc, we consistently observed elevated Dronc protein levels as well as elevated Dronc-dependent caspase activity, and activation in S2 cells where Dnr1 had been depleted prior to induction of apoptosis. Furthermore, overexpression of Dnr1 suppresses apoptosis by an array of inducers. These data indicate that Dnr1 negatively regulates the apoptosis apparatus of S2 cells. We note that Dnr1 does not appear essential for caspase inhibition, because Dnr1 depletion does not result in massive cell death in tissue culture assays. These data suggest that Dnr1 partially suppresses apoptotic caspase activity in *Drosophila*. In this regard, Dnr1 bears similarities to DIAP2. Deletion of DIAP2 from S2 cells also results in a moderate elevation of caspase activity and a recent study demonstrated that overexpression of DIAP2 inhibits apoptosis in vivo (Leulier et al., 2006; Zimmermann et al., 2002).

Our in vitro data suggest that Dnr1 inhibits Dronc, at least partially, by inducing depletion of Dronc protein levels – although we do not rule out parallel mechanisms. Analysis of various Dnr1 deletion constructs indicated that the RING domain is essential for Dronc destruction, suggesting that Dnr1 targets Dronc for proteasomal degradation. We also confirmed that the RING domain has a large impact on Dnr1 autoregulation, because point mutations or deletions that affect the RING domain result in considerable stabilization of the protein. These observations are similar to previous reports demonstrating DIAP1 auto-ubiquitylation and ubiquitylation of Dronc (Wilson et al., 2002; Yoo et al., 2002). Interestingly, we demonstrated that subcellular localization determinants also contribute to Dnr1 stability and Dnr1-mediated destruction of Dronc. N-terminal deletions that remove the FERM domain in Dnr1 block destruction of Dronc. Likewise, removal of the FERM motif and adjacent NLS greatly stabilizes Dnr1, despite the presence of an intact C-terminal RING domain. Our data also reveal differences in the structural requirements on Dnr1 for autoregulation and Dronc destruction. Whereas amino acids 324-397 appear dispensable for regulation of Dronc protein levels, loss of the RING domain greatly stabilizes Dnr1.

Although we consistently observed several interactions between Dnr1 and Dronc, Dnr1 appeared to have no effect on Drice protein levels (data not shown). Thus, we reasoned that Dnr1 is a specific inhibitor of initiator caspases. As initiator caspases are characterized by large N-terminal pro-domains, we speculated that Dnr1 recognizes a structural feature of the pro-domain to regulate Dronc protein levels. We tested whether Dnr1-mediated depletion of Dronc required a pro-domain on Dronc. Surprisingly, our cell culture data indicated that this is not the case. This is further supported by our observation that the apoptotic Pr2 isoform of Dronc, which lacks the pro-domain, is more stable in S2 cells lacking Dnr1. Thus, we assume that Dnr1 recognizes a feature of the enzymatic portion of initiator caspases.

A noteworthy feature of our results is that both wild-type and RING-domain-inactive versions of Dnr1 blocked apoptosis induced by RNAi of DIAP1. This is in contrast to the situation with apoptosis induced by cytotoxic agents where a RING-domain-inactive version of Dnr1 fails to block apoptosis. These apparently conflicting data are similar to previous reports on RING-domain involvement in DIAP1 activity. Whereas, RING-domain mutations of *diap1* are embryonic lethal (Goyal et al., 2000; Lisi et al., 2000; Wang et al., 1999; Yoo et al., 2002) there are several reported situations where the RING domain is not necessary to block apoptosis. For example, a previous report demonstrated that a RING-domain inactive version of DIAP1 blocks Hid-mediated induction of apoptosis in S2 cells where endogenous DIAP1 has been removed by RNAi (Yokokura et al., 2004). Similarly, RING-domain mutations in DIAP1 are less sensitive to apoptosis induced by Hid in vivo (Lisi et al., 2000; Wilson et al., 2002). Thus, it is clear that, whereas the RING domain of DIAP1 is essential for faithful execution of the embryonic developmental program, it is not necessary to silence all apoptotic triggers. These differences probably reflect fundamental differences in the form of caspase activation mediated by the individual triggers. A comparable situation has been broadly documented in higher eukaryotes where investigators distinguish intrinsic and extrinsic apoptotic pathways. In the extrinsic pathway, external signals, such as TNF-α binding its cognate receptor, induce the formation of a caspase-8-containing macromolecular complex that initiates apoptosis. By contrast, intrinsic signals, such as extensive DNA damage trigger caspase-9-bearing apoptosome assembly and subsequent apoptosis in the intrinsic pathway. It is clear that these distinct pathways present equally distinct interfaces for apoptosis-regulating molecules to interact with. Likewise, we propose that cytotoxic agents or genetic triggers, such as dsRNA targeting *diap1* induce apoptosis in fundamentally distinct manners in *Drosophila* assays. In this model, Dnr1 interacts with the apoptotic apparatus in a RING-domain-dependent manner to block Dronc (and potentially other substrates) in response to cytotoxic stress, whereas RNAi of DIAP1 manifests itself as a distinct apoptotic apparatus that interacts with Dnr1 in a different and RING-domain-independent manner. We are presently generating a series of transgenic and mutant Dnr1 lines to investigate these questions in the context of a whole organism. Interestingly, our preliminary data shows that ubiquitous expression of Dnr1 in the developing eye partially suppresses apoptosis induced by coexpression of Hid in the morphogenetic furrow (data not shown).

Materials and Methods

S2 cell culture

S2 cells were maintained at 25°C in Schneider's *Drosophila* medium (GIBCO) supplemented with 10% heat-inactivated fetal calf serum, penicillin and streptomycin. For induction of apoptosis S2 cells were incubated in 1 μM actinomycin D (Sigma) or 25 μg/ml cycloheximide (Sigma) for 6 hours at 25°C or placed on a UV transilluminator for 5 minutes. To determine the apoptotic index, a population of approximately 200 S2 cells was counted and cells were defined as apoptotic if membrane blebbing was visible. The apoptotic index was counted by dividing the number of apoptotic cells by the total number of cells in a given population. Transient transfections were performed using Celfectin Reagent (Invitrogen) according to the manufacturer's instructions. Stable S2 cell lines used in this study were generated according to the Invitrogen *Drosophila* Expression System Protocol using Hygromycin B (Invitrogen) as a selection marker. The dsRNAs and RNAi protocol have been described previously (Foley and O'Farrell, 2004). Primer sequences for generating the dsRNA are available at http://www.ualberta.ca/~efoley/library.html.

Real-time PCR

For real-time PCR analysis total RNA was purified from S2 cells using Trizol (Invitrogen) according to the manufacturers instructions and incubated with DNase. cDNA was prepared from 5 μg purified RNA using oligonucleotode dT primers. Real-time PCR was performed in an Eppendorf realplex2 PCR machine using SyBr green as a detection reagent. The following primers were used to detect the respective transcripts: Actin forward, 5′-TGCCTCATCGCCGACATAA-3′, Actin reverse, 5′-CACGTCACCAGGGCGTAAT-3′; Dcp-1 forward, 5′-ACACGCCGACTTT-CTCTTCT-3′, Dcp-1 reverse, 5′-GATCAGCGATTGCATGTACC-3′; Decay forward, 5′-TGACCTTCTCCGAGATCAAC-3′, Decay reverse, 5′-TTAGCGTAGACCTTGC-CTTC-3′; Dnr1 forward, 5′-ATTCAATGAGTCGTCGCT Dnr1 reverse, 5′-AGCA-CATGCTCCTTCTCCTT-3′. All transcripts were quantified relative to actin levels.

Caspase activity assays

Caspase activity was measured using fluorogenic AMC-labeled caspase peptide substrates (DEVD, YEVD, VEID, IETD, LEHD). S2 cells were pellet at 1000 ***g*** for 3 minutes, washed in PBS and lysed in lysis buffer [10 mM Tris (pH 7.4), 10 mM NaH_2PO_4, 150 mM NaCl, 1% Triton X-100] on ice for 10 minutes. 100 μg lysate was incubated with 50 μM of the respective AMC-labeled caspase substrates in a final volume of 100 μl reaction buffer [10 mM HEPES (pH 7.5), 50 mM NaCl, 0.5 mM EDTA (pH 8.0), 0.1% CHAPS, 10% glycerol, 10 mM DTT] and incubated at 37°C for 1 hour. Fluorescence was measured in a Wallac Victor 2 multilable counter.

Western blotting and protein quantification

S2 cells were harvested by centrifugation at 1000 ***g*** for 3 minutes and lysed on ice for 10 minutes in lysis buffer. Lysate was spun for 10 minutes at maximum speed, and the supernatant was added to sample loading buffer. Samples were separated by SDS-PAGE and analyzed by western blotting. Anti-GFP antibody was purchased from BabCO. Mouse monoclonal anti-myc, anti-actin and anti-HA antibodies were purchased from Sigma and rabbit polyclonal anti-active human caspase-3 was purchased from Cell Signaling. The anti-Dronc antibody has been described previously (Muro et al., 2002). Protein quantification on western blots was performed with an Aerius reader (Licor) following the manufacturer's recommendations.

Microscopy, immunofluorescence and image processing

DIC images were captured on a Zeiss Invertoskop 40C microscope using a Canon Powershot S2 IS camera. Time-lapse recordings were performed by capturing images every 4 minutes over a 16-hour period. Confocal images were captured on a Zeiss LSM 510 confocal microscope using LSM 5 software. S2 cells were deposited on Superfrost Plus Gold slides (Fisher Scientific) for immunofluorescence. Cells were fixed for 5 minutes in 4% formaldehyde (Sigma). DNA was visualized with Hoechst 33258, actin was visualized with Alexa Fluor-568-coupled phalloidin and the nuclear envelope was visualized with Alexa Fluor-568-coupled wheat germ agglutinin (all from Molecular Probes). Images were processed with Adobe Photoshop 8.0, and figures were assembled with Adobe Illustrator 11.0.

Generation of expression constructs for S2 cells

The HADnr1 and HADnr1C563Y expression plasmids have been described previously (Foley and O'Farrell, 2004). MTDnr1 and MTDnr1C563Y were generated by cloning the respective HADnr1 variants as *Kpn*I-*Xba*I fragments into pMT/V5-HisB (Invitrogen). All other tagged expression constructs were generated using the Gateway recombination system (Invitrogen, Gateway vectors purchased from the DGRC). PCR fragments corresponding to the individual Dronc or Dnr1 constructs were TOPO cloned into pENTR/D-TOPO (Invitrogen). The DroncΔPro construct encodes Dronc without the N-terminal 103 amino acids. Table 1 lists the primers used to generate the individual pENTR/D-TOPO constructs.

We are grateful to David Bond, Debby Burshtyn and Michele Barry for critical reading of the manuscript. Bruce Hay provided anti-Dronc and anti-Drice antibodies. John Abrams provided *Dronc* DNA. Gateway vectors were purchased from the *Drosophila* Genomics Resource Center (DGRC). This work was funded by an operating grant from the Canadian Institutes for Health Research. E.F. is a Scholar of the Alberta Heritage Foundation for Medical Research and holds a Canada Research Chair in Innate Immunity.

References

Arama, E., Agapite, J. and Steller, H. (2003). Caspase activity and a specific cytochrome C are required for sperm differentiation in Drosophila. *Dev. Cell* **4**, 687-697.

Baehrecke, E. H. (2002). How death shapes life during development. *Nat. Rev. Mol. Cell Biol.* **3**, 779-787.

Chai, J., Yan, N., Huh, J. R., Wu, J. W., Li, W., Hay, B. A. and Shi, Y. (2003). Molecular mechanism of Reaper-Grim-Hid-mediated suppression of DIAP1-dependent Dronc ubiquitination. *Nat. Struct. Biol.* **10**, 892-898.

Chen, P., Nordstrom, W., Gish, B. and Abrams, J. M. (1996). grim, a novel cell death gene in Drosophila. *Genes Dev.* **10**, 1773-1782.

Chen, P., Ho, S. I., Shi, Z. and Abrams, J. M. (2004). Bifunctional killing activity encoded by conserved reaper proteins. *Cell Death Differ.* **11**, 704-713.
Chew, S. K., Akdemir, F., Chen, P., Lu, W. J., Mills, K., Daish, T., Kumar, S., Rodriguez, A. and Abrams, J. M. (2004). The apical caspase dronc governs programmed and unprogrammed cell death in Drosophila. *Dev. Cell* **7**, 897-907.
Chun, H. J., Zheng, L., Ahmad, M., Wang, J., Speirs, C. K., Siegel, R. M., Dale, J. K., Puck, J., Davis, J., Hall, C. G. et al. (2002). Pleiotropic defects in lymphocyte activation caused by caspase-8 mutations lead to human immunodeficiency. *Nature* **419**, 395-399.
Daish, T. J., Mills, K. and Kumar, S. (2004). Drosophila caspase DRONC is required for specific developmental cell death pathways and stress-induced apoptosis. *Dev. Cell* **7**, 909-915.
Deveraux, Q. L. and Reed, J. C. (1999). IAP family proteins – suppressors of apoptosis. *Genes Dev.* **13**, 239-252.
Dorstyn, L., Colussi, P. A., Quinn, L. M., Richardson, H. and Kumar, S. (1999). DRONC, an ecdysone-inducible Drosophila caspase. *Proc. Natl. Acad. Sci. USA* **96**, 4307-4312.
Foley, E. and O'Farrell, P. H. (2004). Functional dissection of an innate immune response by a genome-wide RNAi screen. *PLoS Biol.* **2**, E203.
Fraser, A. G. (1999). Programmed cell death in C. elegans. *Cancer Metastasis Rev.* **18**, 285-294.
Fraser, A. G. and Evan, G. I. (1997). Identification of a Drosophila melanogaster ICE/CED-3-related protease, drICE. *EMBO J.* **16**, 2805-2813.
Fraser, A. G., McCarthy, N. J. and Evan, G. I. (1997). drICE is an essential caspase required for apoptotic activity in Drosophila cells. *EMBO J.* **16**, 6192-6199.
Goyal, L., McCall, K., Agapite, J., Hartwieg, E. and Steller, H. (2000). Induction of apoptosis by Drosophila reaper, hid and grim through inhibition of IAP function. *EMBO J.* **19**, 589-597.
Green, D. R. and Evan, G. I. (2002). A matter of life and death. *Cancer Cell* **1**, 19-30.
Grether, M. E., Abrams, J. M., Agapite, J., White, K. and Steller, H. (1995). The head involution defective gene of Drosophila melanogaster functions in programmed cell death. *Genes Dev.* **9**, 1694-1708.
Hay, B. A. (2000). Understanding IAP function and regulation: a view from Drosophila. *Cell Death Differ.* **7**, 1045-1056.
Hay, B. A. and Guo, M. (2006). Caspase-dependent cell death in Drosophila. *Annu. Rev. Cell Dev. Biol.* **22**, 623-650.
Hay, B. A., Wassarman, D. A. and Rubin, G. M. (1995). Drosophila homologs of baculovirus inhibitor of apoptosis proteins function to block cell death. *Cell* **83**, 1253-1262.
Horvitz, H. R. (1999). Genetic control of programmed cell death in the nematode Caenorhabditis elegans. *Cancer Res.* **59**, 1701s-1706s.
Huh, J. R., Vernooy, S. Y., Yu, H., Yan, N., Shi, Y., Guo, M. and Hay, B. A. (2004). Multiple apoptotic caspase cascades are required in nonapoptotic roles for Drosophila spermatid individualization. *PLoS Biol.* **2**, E15.
Jacobson, M. D., Weil, M. and Raff, M. C. (1997). Programmed cell death in animal development. *Cell* **88**, 347-354.
Kaiser, W. J., Vucic, D. and Miller, L. K. (1998). The Drosophila inhibitor of apoptosis D-IAP1 suppresses cell death induced by the caspase drICE. *FEBS Lett.* **440**, 243-248.
Kanuka, H., Sawamoto, K., Inohara, N., Matsuno, K., Okano, H. and Miura, M. (1999). Control of the cell death pathway by Dapaf-1, a Drosophila Apaf-1/CED-4-related caspase activator. *Mol. Cell* **4**, 757-769.
Kiessling, S. and Green, D. R. (2006). Cell survival and proliferation in Drosophila S2 cells following apoptotic stress in the absence of the APAF-1 homolog, ARK, or downstream caspases. *Apoptosis* **11**, 497-507.
Kilpatrick, Z. E., Cakouros, D. and Kumar, S. (2005). Ecdysone-mediated up-regulation of the effector caspase DRICE is required for hormone-dependent apoptosis in Drosophila cells. *J. Biol. Chem.* **280**, 11981-11986.
Leulier, F., Rodriguez, A., Khush, R. S., Abrams, J. M. and Lemaitre, B. (2000). The Drosophila caspase Dredd is required to resist gram-negative bacterial infection. *EMBO Rep.* **1**, 353-358.
Leulier, F., Ribeiro, P. S., Palmer, E., Tenev, T., Takahashi, K., Robertson, D., Zachariou, A., Pichaud, F., Ueda, R. and Meier, P. (2006). Systematic in vivo RNAi analysis of putative components of the Drosophila cell death machinery. *Cell Death Differ.* **13**, 1663-1674.
Li, P., Nijhawan, D., Budihardjo, I., Srinivasula, S. M., Ahmad, M., Alnemri, E. S. and Wang, X. (1997). Cytochrome c and dATP-dependent formation of Apaf-1/caspase-9 complex initiates an apoptotic protease cascade. *Cell* **91**, 479-489.
Lisi, S., Mazzon, I. and White, K. (2000). Diverse domains of THREAD/DIAP1 are required to inhibit apoptosis induced by REAPER and HID in Drosophila. *Genetics* **154**, 669-678.
McDonald, E. R., 3rd and El-Deiry, W. S. (2004). Suppression of caspase-8- and -10-associated RING proteins results in sensitization to death ligands and inhibition of tumor cell growth. *Proc. Natl. Acad. Sci. USA* **101**, 6170-6175.
Meier, P., Silke, J., Leevers, S. J. and Evan, G. I. (2000). The Drosophila caspase DRONC is regulated by DIAP1. *EMBO J.* **19**, 598-611.
Mills, K., Daish, T., Harvey, K. F., Pfleger, C. M., Hariharan, I. K. and Kumar, S. (2006). The Drosophila melanogaster Apaf-1 homologue ARK is required for most, but not all, programmed cell death. *J. Cell Biol.* **172**, 809-815.
Muro, I., Hay, B. A. and Clem, R. J. (2002). The Drosophila DIAP1 protein is required to prevent accumulation of a continuously generated, processed form of the apical caspase DRONC. *J. Biol. Chem.* **277**, 49644-49650.
Muro, I., Monser, K. and Clem, R. J. (2004). Mechanism of Dronc activation in Drosophila cells. *J. Cell Sci.* **117**, 5035-5041.
Muro, I., Berry, D. L., Huh, J. R., Chen, C. H., Huang, H., Yoo, S. J., Guo, M., Baehrecke, E. H. and Hay, B. A. (2006). The Drosophila caspase Ice is important for many apoptotic cell deaths and for spermatid individualization, a nonapoptotic process. *Development* **133**, 3305-3315.
Opferman, J. T. and Korsmeyer, S. J. (2003). Apoptosis in the development and maintenance of the immune system. *Nat. Immunol.* **4**, 410-415.
Quinn, L. M., Dorstyn, L., Mills, K., Colussi, P. A., Chen, P., Coombe, M., Abrams, J., Kumar, S. and Richardson, H. (2000). An essential role for the caspase dronc in developmentally programmed cell death in Drosophila. *J. Biol. Chem.* **275**, 40416-40424.
Raff, M. C. (1992). Social controls on cell survival and cell death. *Nature* **356**, 397-400.
Rodriguez, A., Oliver, H., Zou, H., Chen, P., Wang, X. and Abrams, J. M. (1999). Dark is a Drosophila homologue of Apaf-1/CED-4 and functions in an evolutionarily conserved death pathway. *Nat. Cell Biol.* **1**, 272-279.
Rodriguez, A., Chen, P., Oliver, H. and Abrams, J. M. (2002). Unrestrained caspase-dependent cell death caused by loss of Diap1 function requires the Drosophila Apaf-1 homolog, Dark. *EMBO J.* **21**, 2189-2197.
Rodriguez, J. and Lazebnik, Y. (1999). Caspase-9 and APAF-1 form an active holoenzyme. *Genes Dev.* **13**, 3179-3184.
Saleh, A., Srinivasula, S. M., Acharya, S., Fishel, R. and Alnemri, E. S. (1999). Cytochrome c and dATP-mediated oligomerization of Apaf-1 is a prerequisite for procaspase-9 activation. *J. Biol. Chem.* **274**, 17941-17945.
Salmena, L., Lemmers, B., Hakem, A., Matysiak-Zablocki, E., Murakami, K., Au, P. Y., Berry, D. M., Tamblyn, L., Shehabeldin, A., Migon, E. et al. (2003). Essential role for caspase 8 in T-cell homeostasis and T-cell-mediated immunity. *Genes Dev.* **17**, 883-895.
Shi, Y. (2002). Mechanisms of caspase activation and inhibition during apoptosis. *Mol. Cell* **9**, 459-470.
Stoven, S., Ando, I., Kadalayil, L., Engstrom, Y. and Hultmark, D. (2000). Activation of the Drosophila NF-kappaB factor Relish by rapid endoproteolytic cleavage. *EMBO Rep.* **1**, 347-352.
Stoven, S., Silverman, N., Junell, A., Hedengren-Olcott, M., Erturk, D., Engstrom, Y., Maniatis, T. and Hultmark, D. (2003). Caspase-mediated processing of the Drosophila NF-kappaB factor Relish. *Proc. Natl. Acad. Sci. USA* **100**, 5991-5996.
Su, H., Bidere, N., Zheng, L., Cubre, A., Sakai, K., Dale, J., Salmena, L., Hakem, R., Straus, S. and Lenardo, M. (2005). Requirement for caspase-8 in NF-kappaB activation by antigen receptor. *Science* **307**, 1465-1468.
Thompson, C. B. (1995). Apoptosis in the pathogenesis and treatment of disease. *Science* **267**, 1456-1462.
Vaux, D. L. and Korsmeyer, S. J. (1999). Cell death in development. *Cell* **96**, 245-254.
Vaux, D. L. and Flavell, R. A. (2000). Apoptosis genes and autoimmunity. *Curr. Opin. Immunol.* **12**, 719-724.
Vaux, D. L. and Silke, J. (2005). IAPs, RINGs and ubiquitylation. *Nat. Rev. Mol. Cell Biol.* **6**, 287-297.
Vucic, D., Kaiser, W. J. and Miller, L. K. (1998). Inhibitor of apoptosis proteins physically interact with and block apoptosis induced by Drosophila proteins HID and GRIM. *Mol. Cell Biol.* **18**, 3300-3309.
Wang, S. L., Hawkins, C. J., Yoo, S. J., Muller, H. A. and Hay, B. A. (1999). The Drosophila caspase inhibitor DIAP1 is essential for cell survival and is negatively regulated by HID. *Cell* **98**, 453-463.
White, K., Grether, M. E., Abrams, J. M., Young, L., Farrell, K. and Steller, H. (1994). Genetic control of programmed cell death in Drosophila. *Science* **264**, 677-683.
White, K., Tahaoglu, E. and Steller, H. (1996). Cell killing by the Drosophila gene reaper. *Science* **271**, 805-807.
Wilson, R., Goyal, L., Ditzel, M., Zachariou, A., Baker, D. A., Agapite, J., Steller, H. and Meier, P. (2002). The DIAP1 RING finger mediates ubiquitination of Dronc and is indispensable for regulating apoptosis. *Nat. Cell Biol.* **4**, 445-450.
Xu, D., Li, Y., Arcaro, M., Lackey, M. and Bergmann, A. (2005). The CARD-carrying caspase Dronc is essential for most, but not all, developmental cell death in Drosophila. *Development* **132**, 2125-2134.
Xu, D., Wang, Y., Willecke, R., Chen, Z., Ding, T. and Bergmann, A. (2006). The effector caspases drICE and dcp-1 have partially overlapping functions in the apoptotic pathway in Drosophila. *Cell Death Differ.* **13**, 1697-1706.
Yokokura, T., Dresnek, D., Huseinovic, N., Lisi, S., Abdelwahid, E., Bangs, P. and White, K. (2004). Dissection of DIAP1 functional domains via a mutant replacement strategy. *J. Biol. Chem.* **279**, 52603-52612.
Yoo, S. J., Huh, J. R., Muro, I., Yu, H., Wang, L., Wang, S. L., Feldman, R. M., Clem, R. J., Muller, H. A. and Hay, B. A. (2002). Hid, Rpr and Grim negatively regulate DIAP1 levels through distinct mechanisms. *Nat. Cell Biol.* **4**, 416-424.
Yu, S. Y., Yoo, S. J., Yang, L., Zapata, C., Srinivasan, A., Hay, B. A. and Baker, N. E. (2002). A pathway of signals regulating effector and initiator caspases in the developing Drosophila eye. *Development* **129**, 3269-3278.
Yuan, J. and Yankner, B. A. (2000). Apoptosis in the nervous system. *Nature* **407**, 802-809.
Yuan, J., Shaham, S., Ledoux, S., Ellis, H. M. and Horvitz, H. R. (1993). The C. elegans cell death gene ced-3 encodes a protein similar to mammalian interleukin-1 beta-converting enzyme. *Cell* **75**, 641-652.
Zachariou, A., Tenev, T., Goyal, L., Agapite, J., Steller, H. and Meier, P. (2003). IAP-antagonists exhibit non-redundant modes of action through differential DIAP1 binding. *EMBO J.* **22**, 6642-6652.
Zhou, L., Song, Z., Tittel, J. and Steller, H. (1999). HAC-1, a Drosophila homolog of APAF-1 and CED-4 functions in developmental and radiation-induced apoptosis. *Mol. Cell* **4**, 745-755.
Zimmermann, K. C., Ricci, J. E., Droin, N. M. and Green, D. R. (2002). The role of ARK in stress-induced apoptosis in Drosophila cells. *J. Cell Biol.* **156**, 1077-1087.
Zou, H., Li, Y., Liu, X. and Wang, X. (1999). An APAF-1.cytochrome c multimeric complex is a functional apoptosome that activates procaspase-9. *J. Biol. Chem.* **274**, 11549-11556.